Nonideal regimes of deflagration and detonation of black powder

5 authors, including:

Boris Ermolaev
Semenov Institute of Chemical Physics
71 PUBLICATIONS   293 CITATIONS

SEE PROFILE

K. A. Sleptsov
Federal Service for Supervision in the Sphere of Science and Education
2 PUBLICATIONS   7 CITATIONS

SEE PROFILE

Some of the authors of this publication are also working on these related projects:

Convective burning and explosion in mixtured explosive systems View project

COMBUSTION, EXPLOSION, AND SHOCK WAVES

Nonideal Regimes of Deflagration and Detonation of Black Powder

B. S. Ermolaev[a], A. A. Belyaev[a], S. B. Viktorov[b], K. A. Sleptsov[b], and S. Yu. Zharikova[b]

[a] *Semenov Institute of Chemical Physics, Russian Academy of Sciences, Moscow, 119991 Russia*
[b] *Moscow State Engineering Physics Institute, Moscow, 115409 Russia*
e-mail: boris.ermolaev@yahoo.com
Received February 9, 2009

Abstract—The explosive and deflagration properties of black powder differ significantly from those of modern propellants and compositions based on ammonium nitrate or ammonium perchlorate. Possessing a high combustibility, black powder is capable of maintaining stable combustion at high velocities in various shells, be it steel shells or thin-walled plastic tubes, without experiencing deflagration-to-detonation transition. It is extremely difficult to detonate black powder, even using a powerful booster detonator. The results of numerical simulations of a number of key experiments on the convective combustion and shock initiation of black powder described in the literature are presented. The calculations were performed within the framework of a model developed previously for describing the convective combustion of granulated pyroxylin powders, with small modifications being introduced to allow for the specific properties of black powder. The thermophysical properties of the products of combustion and detonation and the parameters of the equation of state of black powder were determined from thermodynamic calculations. The calculation results were found to be in close agreement with the experimental data. The simulation results were used to analyze the regularities of the wave processes in the system and their relation to the properties of black powder and the experimental conditions. It was demonstrated that the effects observed could be explained by a weak dependence of the burning rate of black powder on the pressure.

INTRODUCTION

Black powder is an energetic material prepared by mechanical mixing of potassium nitrate, sulfur, and charcoal in a proportion of about 75 : 10 : 15 wt %. It is readily ignited and burns at a high rate. The combustion products contain a large amount of condensed phase, a factor that makes them incendiary. The literature on black powder dates back to the ancient times. Here, we will limit ourselves to mentioning only key monographs [1, 2] and a few original studies [3–7] the results of which will be used in the present work.

Being a precursor of modern composite propellants and explosive compositions, black powder, nevertheless, differs from them drastically, demonstrating rather unusual, mostly inexplicable behavior during deflagration and detonation. First, in contrast to explosive compositions based on ammonium nitrate and ammonium perchlorate, black powder exhibits no deflagration-to-detonation transition. Even in long, strong tubes, the burning velocity does not exceed 400–440 m/s [7]. Upon shock initiation, two different processes with stable characteristics are observed: a combustion wave propagating at a velocity of ~400 m/s (as in the case of thermal initiation!) and a combustion wave propagating at a velocity of 1100–1300 m/s, which was termed detonation [4]. Experiments with charges placed into long, thin-walled, low-strength tubes demonstrated the unique ability of black powder

to sustain a fast burning in a quasi-steady pulsating regime with periodic local ruptures of the shell [5].

The present work is devoted to a theoretical analysis of the properties of black powder and their interpretation based on the modern concepts of deflagration and detonation. For this analysis, we selected several typical experiments and tried to reproduce their results in numerical simulations. A detailed description of these experiments is given in [4–7]. A brief summary of the experimental data is presented along with the results of numerical simulations in the relevant sections.

THEORETICAL FORMULATION OF THE PROBLEM

The theoretical model and computer code were largely developed in [8] for studying the convective combustion of granular gun-cotton powder [8]. The model was developed in a one-dimensional approximation within the framework of the mechanics of two-phase (gas–powder) reacting mixtures; in its basic aspects, it was similar to the analogous model extensively discussed in the literature (see, e.g., [9]). The model was adapted to black powder by introducing minor changes. Here, we will present only a brief description of the model and changes made, referring the reader for more details to [8], where the main con-

cept underlying the model, flow equations, and computer code are presented.

Consider a charge composed of spherical powder grains of the same size in a cylindrical shell with closed ends. The input parameters of the problem specify the powder granule size, porosity, length and diameter of the charge, and shell wall thickness, as well as the temperature, pressure, and density of the gas occupying the pore space. In the experiments, the powder charge was initiated by an electrically heated spiral or by a booster detonator. In the model, initiation was imitated by starting the burning of a thin layer of black powder or by blowing hot gas through the end face of the charge at a preset rate for a preset time, with the latter variant providing explosive initiation.

The system of equations describing the flow of a two-phase reacting mixture consists of the differential equations of conservation of mass, momentum, and energy for the gas phase (combustion products) and solid phase (powder grains), as well as the equations of state for the phases and the equations for intergranular stresses. Intergranular stresses arise because of viscoplastic deformations during the densification of the granular layer and contribute to the pressure in the solid phase. The conservation equations in partial derivatives were written in the quasi-one-dimensional approximation with consideration given to the expansion of the current tube due to a possible lateral expansion of the charge shell. The gas and solid phases of the reacting mixture have different density, internal energy (temperature), pressure, flow velocity, and volume fraction. The equation of state of the combustion products can be written in an arbitrary form capable of approximating the results of thermodynamic calculations. It was assumed that the density of black powder depends only on the pressure (Tait equation with two coefficients: the bulk modulus and pressure exponent). The dependence of the powder density on the temperature was disregarded. This simplification, acceptable for the problems under consideration makes it possible to exclude the energy conservation equation for the solid phase from the system of equations describing the two-phase reacting flow.

The burning of powder grains and the difference in the velocities of motion of the phases are the driving forces of the interphase transfer of mass, momentum, and energy. The intensity of this transfer is calculated based on correlation dependences approximating experimental data on the resistance coefficient and Nusselt number for flows in porous layers. The intensity of interphase mass transfer is calculated as the product of the specific surface area of powder grains and the layer-by-layer burning rate; the latter quantity is specified as an empirical function of the pressure.

A powder granule was assumed to begin to burn when the temperature of its surface reached the ignition temperature T_{ig}, which was set constant. The temperature of the surface of a powder granule changes due to convective heat transfer from the hot gas, dissipative heating originating from viscoplastic deformations during the densification of the layer of powder grains, and thermal conduction from the surface into the bulk of the granule. These processes were simulated using elementary cells, which were specified at each point along the charge length ahead of the combustion front. The cell was thought of as a tube, with a diameter and wall thickness calculated based on the local values of the powder granule diameter and porosity. To calculate the cell wall thickness, it is necessary to solve the heat conduction equation with account of internal dissipative heat sources. The heat flux at the surface of the channel of the cell, the change of its diameter, and the intensity of dissipative processes were calculated based on the local characteristics of the two-phase medium. At the instant of time when the channel surface temperature reaches T_{ig}, the process of heating gives way to combustion.

The deformation and disintegration of the shell of the charge was treated approximately in two different variants. For a thick-walled cylindrical shell made of strong steel, a local lateral expansion begins when the pressure exceeds a threshold value, which is determined by the yield stress of the shell material and by the ratio of the shell thickness to the channel diameter. The material experiencing deformation is treated as an ideally plastic substance. For a weak, thin-walled shell fabricated of a readily deformable material (plastic or brass), we took into account elastic deformations and assumed that, at a spot where the pressure generated by the combustion wave exceeds the shell strength, a hole is formed. The destruction of the shell is of fragile character, beginning from the formation of a longitudinal through crack. Upon spreading throughout the region of high pressure gives rise to transverse cracks, which eventually transform into a hole. A mixture of hot combustion products and burning powder grains are ejected through the hole into the ambient medium.

The problem was solved numerically by using an implicit finite difference scheme in combination with the tridiagonal matrix algorithm and by introducing splitting into a macroscale (the conservation equations for a two-phase flow) and a mesoscale (heat conduction equation). We employed an adaptive computational grid along the charge length, uniform at the initial moment but becoming finer (coarser) with increasing (decreasing) gradients of the dependent variables in the course of calculations. The computational grid across the thickness of the cell vault at the mesoscale was attached to the internal boundary of the cell and had a step that increased in geometric progression with the distance from this boundary. Application of the model to black powder needs the following clarifications. Although the products of combustion of black powder contain 50 wt % of condensed particles, the model postulates that all the products are gaseous. This means that the particles are so small that the deviations of their temperature and velocity from

Table 1. Results of the thermodynamic calculations of the characteristics of the Chapman–Jouguet detonation of black powder

Initial density, kg/m^3	Detonation velocity, m/s	Detonation pressure, GPa	Tempe-rature, K	Density of products, kg/m^3	Speed of sound, m/s	Particle velocity, m/s	$\gamma = C_p/C_v$	Gaseous products, wt %	Liquid-drop-let products, wt %
200	1223	0.13	2542	350	700	523	1.13	49	51
400	1422	0.29	2568	630	907	515	1.105	48.8	51.2
600	1685	0.53	2591	870	1160	525	1.103	48.7	51.3
800	2031	0.89	2612	1090	1500	531	1.101	48.75	51.25
1000	2482	1.45	2633	1310	1900	582	1.10	48.75	51.25

those of the gas are negligibly small. To implement the model, it is necessary to know the properties of this pseudogas, in particular, its equation of state in the form of the dependence of the pressure P on the density ρ_g and internal energy of the products e_g. The thermodynamic properties and chemical composition of the products at elevated pressures were determined from the results of thermodynamic equilibrium calculations by using the TDS code [10−12]. This code calculates theoretical equations of state from Exp-6 intermolecular potentials within the framework of the modern apparatus of statistical mechanics, which makes it possible to realistically describe the thermodynamic characteristics of complex chemically reacting system over wide ranges of temperatures and pressures, including the parameters of detonation of high explosives. The calculation results for black powder are presented below.

In our model, the equation of state of the products was presented by a two-term analytical expression [13] similar to the Mie−Grüneisen equation:

$$P = (\gamma - 1)\rho_g e_g + B_g \rho_g^m \left(\frac{m - \gamma}{m - 1} \right). \qquad (1)$$

The three coefficients in Eq. (1) were determined from calibration calculations performed using data on the dependence of the detonation characteristics on the initial density of powder, which, in turn, were calculated with the help of the TDS code (Table 1). The values of $\gamma = 1.11$, $m = 2.8181$, and $B_g = 2.5252$ Pa/(kg m^3)^m provide the best fit to these data.

The presence of condensed particles in the pseudogas causes an increase in the friction resistance and heat transfer coefficient for its flowing through a porous layer. A preliminary analysis shows that the characteristics of this effect can be adequately estimated only if the size of these particles is known, which, however, is not the case. Therefore, we introduced no changes into the correlation relationship used in the model to calculate the friction resistance (in this case, due to a higher density of the pseudogas compared to the pure gas, the intensity of friction was approximately twice as high). Along with the convective term α_{conv}, the heat transfer coefficient included the term associated with heat transfer during the dep-

osition of condensed particles at the surface of powder granules:

$$\alpha_s = \alpha_{conv} + \alpha_{dep}. \qquad (2)$$

The first term was calculated in a standard way, by using the empirical relationship between the Nusselt and Reynolds numbers for the flow of a gas in a porous layer. The second term was defined as the product of the flow velocity, bulk density of condensed particles, their specific heat, and deposition coefficient. Estimates show that the deposition coefficient can be set equal to unity and that the rate of heat transfer via deposition is severalfold higher than that via convection.

The rate of layer-by-layer burning of black powder was measured over wide pressure range, up to 400 MPa [14, 15], although a significant scatter in the high-pressure data was observed. In our calculations, we used Vieille's law, $U_p = BP^n$, with a pressure exponent of $n = 0.22$.

The quasi-static component of the intergranular stresses for black powder was determined in a standard way, from data on static densification of the sample with a press. The calculations were performed using the formula $\sigma = \sigma_m F(\varphi)$, where $\sigma_m = 220$ MPa and $F(\varphi) = (1 - \varphi/0.5)^{2.4}$.

THERMODYNAMIC CHARACTERISTICS OF THE COMBUSTION AND DETONATION OF BLACK POWDER

The experimental studies of the composition of the combustion products of black powder (by sampling) and the combustion characteristics were conducted in a constant-volume bomb nearly a century ago (see [2], the data reported by Abel and Nobel). Averaging and rounding the data presented in different works for gun and cannon black powders with a composition close to the standard one (75% KNO$_3$−10% sulfur−15% wood coal) allowed us to obtain the following results.

The combustion characteristics: the volume of the gas released, 280−290 l/kg; the combustion temperature, somewhat above 2300 K; explosion heat, 2.7−2.9 MJ/kg; and explosive force of powder, 0.28−0.30 MJ/kg [16] (lower values of this parameter, 0.25−0.26 MJ/kg, reported in [2], were probably obtained without allowance for heat loss).

The composition of the combustion products: the gas phase comprises 43−44 wt %, including 26−27 wt % CO_2, ~11% N_2, and 3.5−5.0 wt % CO; the condensed phase comprised 55−56 wt %, including 28−34 wt % K_2CO_3, 7.0−12.5 wt K_2SO_4, 8.0−10.5 wt % K_2S, 4−5 wt % S, and 1.0−1.5% H_2O, which is partially present in black power as natural moisture.

The characteristics of combustion and detonation were calculated using the TDS code [10−12] for a typical black powder without regard for the ash content of wood coal and moisture. The chemical formula of wood coal was selected to be C_6H_2O, as recommended in [1]; the standard enthalpy of formation was set at −100 kJ/mol, which corresponds to an internal energy of black powder at standard atmospheric pressure of −3.83 MJ/kg.

The combustion of black powder in a constant-volume bomb can be interpreted within the framework of a thermodynamic problem of equilibrium conversion of the initial mixture at constant volume and constant internal energy. Calculations performed at the loading density of 100 kg/m³ and standard initial conditions with the use of the equation of state of an ideal gas yielded the following results: the calculated combustion characteristics: the combustion temperature, 2340 K; pressure, 29.7 MPa; mean molar weight of the products, 54.4 g/mol; explosive force of powder, 0.292 MJ/kg; polytropic exponent, 1.1; volume of the gaseous products, 336 l/kg; frozen sound speed, 580 m/s; and specific heat, 1.19 kJ/(kg K).

The calculated composition: the gas phase comprises 54.4 wt %, including 20.3 wt % CO_2, 10.4 wt % N_2, 9.2 wt % CO, 6.0 wt % SO_2, 1.7 wt % S_2, 3.2 wt % KOH, and 2.0 wt % H_2O; the liquid phase comprised 45.6 wt %, including 28 wt % K_2CO_3, 6.9 wt % K_2SO_4, and 10.7 wt % K_2S. When comparing with the experimental data, one should keep in mind that the calculated composition corresponds to the combustion temperature rather than room temperature. Cooling to room temperature makes 10% of the gaseous products (sulfur-containing gases and water vapor) condense, so that the agreement in the fractions of gaseous and condensed products is better.

The thermodynamic calculations of the Chapman−Jouguet detonation parameters of black powder were carried out using the Exp-6 intermolecular potentials for the gaseous products. The database for black powder was extended to include the intermolecular potentials of molecules containing potassium and sulfur. The calculation results for various initial densities of powder are listed in Table 1. Since the detonation products contained about 51 wt % liquid phase, the detonation velocity and pressure were low, 2480 m/s and 1.45 GPa at a charge density of 1000 kg/m³. Note, however, that this detonation velocity is nearly twice as high as the value measured at a similar to density of the charge, 1100−1300 m/s. It will be demonstrated that
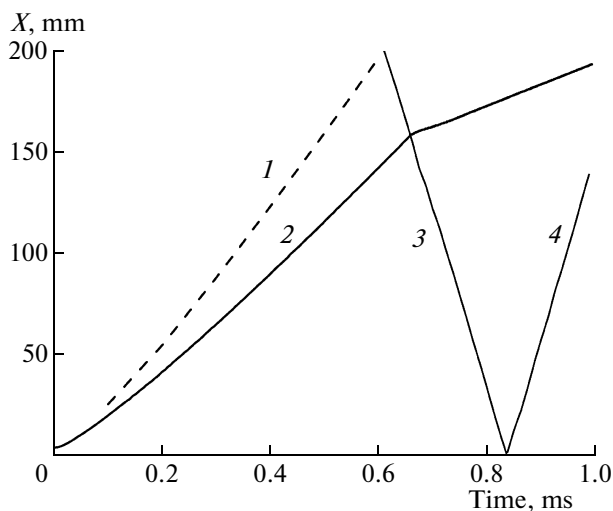

Fig. 1. Trajectories of the fronts for the convective combustion of a 200-mm-long black powder charge: (*1*) plastic deformation wave front propagating at a velocity of 420 m/s; (*2*) combustion wave front propagating at a maximum velocity of 270 m/s; (*3*) pressure wave reflected from the end face (910 m/s), and (*4*) second circulation of the rarefaction wave (940 m/s).

this significant discrepancy is associated with the nonideal character of the real process.

CONVECTIVE COMBUSTION OF A SHORT CHARGE IN A STRONG SHELL

The experiments were performed on a setup that made it possible to obtain slit streak photographs and recordings of the pressure with four piezoelectric transducers located along the axis of the charge [6, 7]. The samples were prepared from the 0.40−0.63-mm fraction of DRP-3 regular black powder. Black powder was poured into the channel of a closed strong shell, 200 mm in length and 5 mm in diameter, and ignited near the closed end by an electrically heated spiral. The measurements made it possible to obtain detailed information on the characteristics of the process, such as the trajectories and velocities of the combustion wave front and of burning powder granules, space and time profiles of the pressure, and the conditions of formation and parameters of the reflected shock wave.

The results are shown in Figs. 1−3. Calculations were performed for a nondeformable shell at a charge density of 1 g/cm³, powder granule diameter of $d_0 = 0.4$ mm, and an ignition temperature of $T_{ig} = 750$ K. The control characteristic was the rate of pressure rise at the transducer located near the ignitor, which was measured to be 200 MPa/ms. To fit the calculation results to the experimental data for this parameter, the constant B in Vieille's law was increased by about a factor of 1.5 compared to the value reported in the literature. Figure 1 shows the trajectories of the combustion wave front, leading edge of plastic deformation
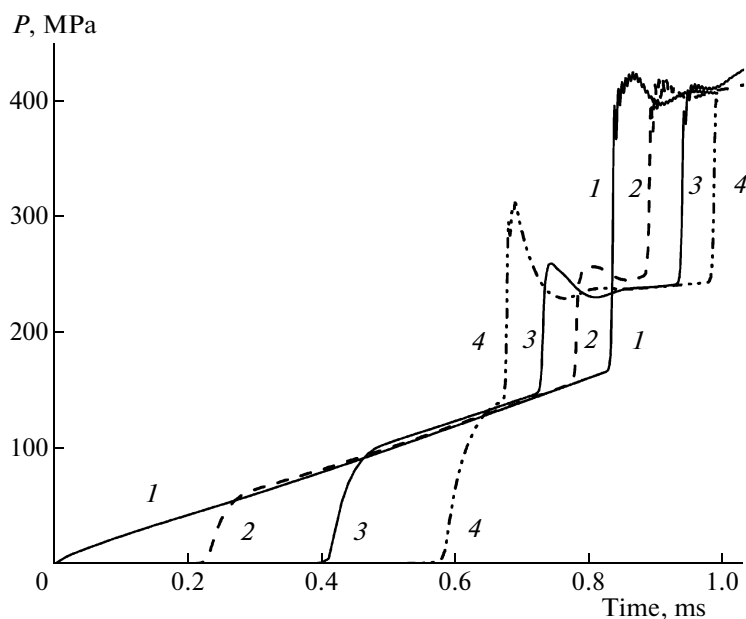
Fig. 2. Time profiles of the pressure at various distances from the end face for the variant specified in Fig. 1 (in mm): (*1*), (*2*) 50, (*3*) 95, and (*4*) 140.
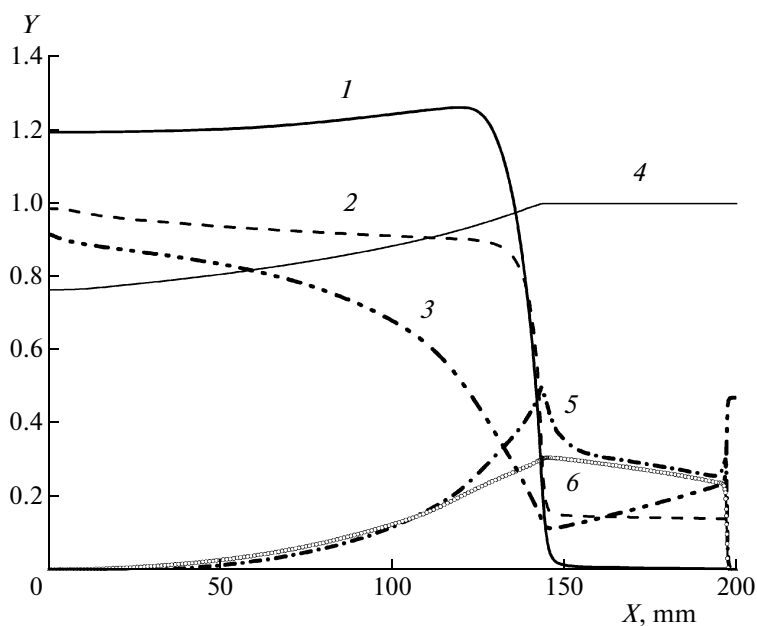

Fig. 3. Space profiles of the key variables for the variant specified in Fig. 1 at a time of 0.6 ms and a combustion front coordinate of 143 mm: (*1*) pressure P divided by 100 MPa, (*2*) internal energy of the gas divided by the heat of explosion of black powder (e_g/Q), (*3*) porosity φ, (*4*) relative diameter of powder granules d/d_0, (*5*) gas velocity U_g divided by 500 m/s, and (*6*) condensed phase velocity U_c divided by 500 m/s.

wave, and two reflected waves, which arise due to the interaction of the flow with the end faces of the charge. After a period of acceleration, the convective combustion wave acquires a constant velocity of 270 m/s. The plastic deformation wave, propagating at a higher velocity (420 m/s as it approaches the end face), outruns the combustion wave front. The reflection of the plastic deformation wave from the closed end face generates a pressure wave, which propagates along the charge in the opposite direction at a velocity of ~900 m/s. This prediction is in a complete agreement with streak photo recordings.

Figure 2 displays the pressure time profiles calculated at four points along the charge length. The calcu-

lated profiles closely reproduce the behavior of the experimental diagrams: the stage of fast pressure growth associated with the passage of the combustion front gives ways to a moderate pressure growth (200 MPa/ms at all transducers), after which the pressure rises sharply again when the reflected shock wave arrives. As in the experiment, the signal from the transducer located 140 mm from the ignition point shows that the moments of passage of the combustion front and arrival of the reflected shock wave are separated only by 30 μs.

Figure 3 shows the coordinate profiles of the key variables at a time of 0.6 ms, when the front is located 143 mm from the ignition point, whereas the leading edge of the plastic-deformation wave approaches the opposite end face of the charge. The structure of the wave is typical of a convective combustion wave [17]. The gas velocity attains its maximum value, 250 m/s, at the combustion front. The velocity of the solid phase flow caused by the formation of a densification zone ahead of the combustion front is as high as 150 m/s, a value close to the measured one.

CONVECTIVE COMBUSTION OF A LONG CHARGE IN A STRONG SHELL

The experiments were performed using black powder charges with a length of up to 2.5 m in strong steel tubes with an inner diameter of 5 and 20 mm. Combustion was initiated with a standard thermal igniter near the closed end face of the tube. The velocity of the combustion wave was measured by photographing the outflow of combustion products through a sequence of small-diameter orifices in the tube wall. Measurements showed that, after a transient segment, 500–600 mm in length, the wave front velocity stopped changing, remaining 400–440 m/s over the rest of the charge length.

The numerical simulations were performed at the same values of the input parameters as in the previous section—only the charge length was increased to 2 m. The calculation results are displayed in Fig. 4: the variation of the combustion wave velocity with the distance along the charge and the space pressure profiles at different moments of time. As can be seen, the calculation results, as the experimental data, suggest that, after attaining a value of 400 m/s within a distance of 700 mm, the combustion wave velocity remains virtually unchanged during the rest of the time, while the maximum pressure in the wave continues to rise.

Figure 5 shows space profiles of the key parameters of the flow at a time of 3 ms over the segment where the front velocity is constant. As compared to the analogous plot for the convective combustion wave in the short charge (Fig. 3), the densification zone is four times longer, 160 mm, whereas the porosity decreases to zero, thereby making the densification zone gas-impenetrable. Despite a relatively high pressure in the
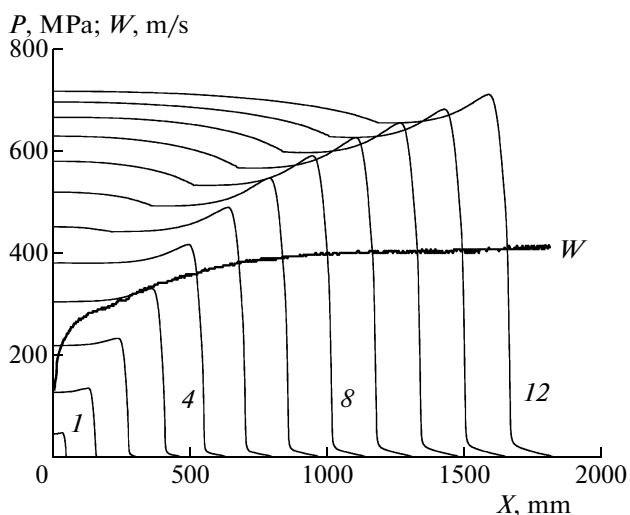

Fig. 4. Variation of the combustion wave front velocity W over the charge length and the space profiles of the pressure at various moments of time (from 0.2 ms (curve *1*) to 4.6 ms (curve *12*) at 0.4 ms intervals).

combustion wave, the plastic-viscous heating in the densification zone is too low to ignite the black powder. Because of a low sensitivity of the burning rate of black powder to the pressure, there exist no conditions for generating secondary waves, an effect underlying one of the mechanisms of convective deflagration-to-detonation transition [18]. All these factors impart stability to a convective combustion wave in black powder, preventing it from explosive acceleration.

Thus, the densification zone formed under the action of intergranular stresses controls the combustion front velocity. This conclusion was supported by special calculations in which the intergranular stress was increased by as a function of 1.5 by varying the constant σ_m. As a result, the steady combustion wave velocity increased to 510 m/s, in agreement with an approximate formula, according to which the plastic-deformation wave is proportional to the square root of the constant σ_m.

SHOCK INITIATION OF A LONG CHARGE IN A STRONG SHELL

It was not until the experiments described in [4] that the shock initiation of black powder produced a combustion wave velocity markedly above 400 m/s. Carefully selecting the experimental conditions (using a booster detonator with suitable properties, a strong shell, and required dispersity), the authors of [4] were able to detonate black powder and realize a steady process propagating at a velocity of 1300 m/s through a 350-mm-long charge. Later, a similar process, but with a somewhat lower velocity (1100 m/s), was initiated in a 1-m-long charge of DRP-3 black powder [7].
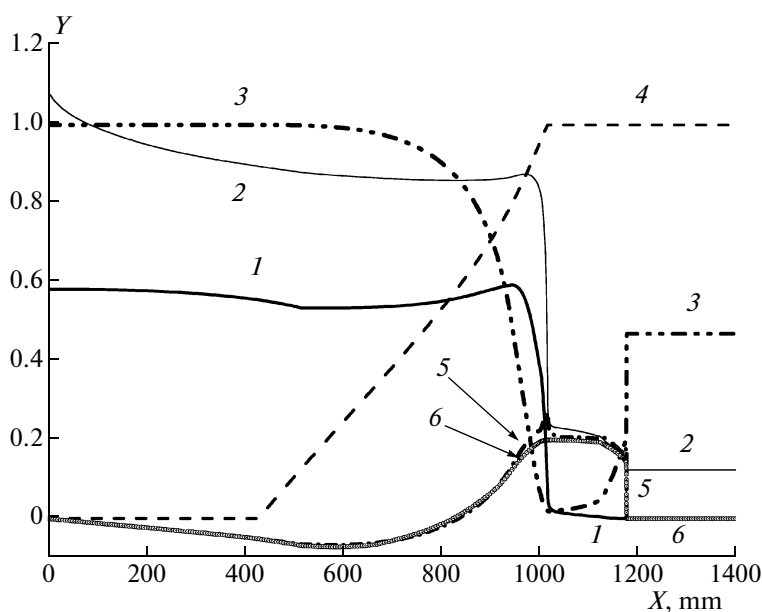
Fig. 5. Space profiles of the key variables for the variant specified in Fig. 4 at a time of 3.0 ms and a combustion front coordinate of 1017 mm: (*1*) P (GPa), (*2*) e_g/Q, (*3*) φ, (*4*) d/d_0, (*5*) U_g (km/s), and (*6*) U_c (km/s).
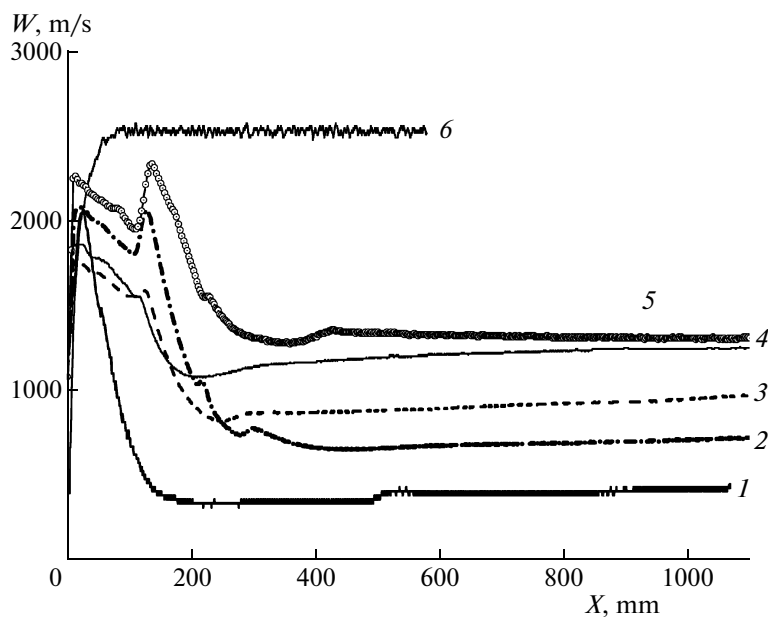

Fig. 6. Combustion front velocity–distance diagram for shock initiation: (*1–5*) numbers of the variants specified in Table 2; (*6*) variant with approaching to the regime of ideal detonation.

In numerical calculations, shock initiation was modeled by a pulsed injection of hot products through the end face of the charge. Selecting the intensity and duration of injection made it possible to change the characteristics of initiation, more specifically, the initial amplitude and velocity of the generated wave.

The calculations were performed for a 1.2-m-long charge. Along with the initiation parameters, we also varied the powder granule diameter d_0. Typical exam-

ples of the time evolution of the front velocity and maximum pressure in the wave are displayed in Figs. 6, 7 (curves *1–5*). The varied parameters and the wave front velocity at the end of the charge are presented in Table 2. In all variants, after the gas inflow stopped, the velocity and pressure in the wave decreased sharply under the action of the rarefaction wave propagating from the end face. This stage of the process occupies 150–300 mm of the charge length. Next, slow relax-

ation occurs, during which the wave velocity achieves nearly constant level, whereas the pressure slowly increases or decreases. The lowest velocity of propagation of steady combustion wave, 410 m/s, was obtained in variant no. 1, for a short gas inflow (30 μs) and a powder granule size of 0.4 mm. As regards its properties and wave front structure, this process is convective combustion with densification wave. It is completely similar to the process that was considered in the previous section (thermal initiation) and had the same velocity.

When the duration and intensity of the pulsed gas inflow was increased and the powder granule size d_0 was decreased to 0.1−0.2 mm, the decay of the velocity and pressure became less deep whereas the velocity of steady propagation increased. For example, for variants 4 and 5, which differ in the conditions of initiation (powder granule size is the same), the combustion wave velocity and the maximum pressure, being drastically different at the initial stage, later markedly converge. The velocities of propagation of the steady wave (1320 and 1250 m/s, respectively) are close to the detonation velocity measured in the experiments with dispersed black powder [4]. However, as can be seen from Fig. 8, which shows the space profiles of the key parameters of the flow at a selected moment of time for variant no. 5, there is a number of indications the wave complex is nonideal. Although the combustion of powder is initiated in the wave front during the compression of the material and the stepwise decrease of the pore volume, a behavior typical of detonation-like processes, the pressure profile has a hump a with maximum located 60 mm behind the wave front, rather than a triangle-shaped von Neumann spike. Note that the pressure at the maximum is nearly twice as high as that at the wave front. Note also that the wave velocity is two times lower than the thermodynamically calculated velocity of the ideal detonation of black powder. Lastly, one can see that the reaction zone thickness, defined as the distance from the wave front to the point at which the powder granule diameter becomes zero, is 400 mm, a very large value—only three times smaller than the charge length. Recall that the measurement base in experiments on the determination of the velocity of the steady detonation of secondary high explosives exceeds by a factor of tens or even hundreds the thickness of the reaction zone of the detonation wave. Thus, to allow the wave to complete its evolution, the length of a black powder charge should be at least several times large than those used in the calculations and experiments. It would be interesting to numerically simulate an ideal detonation wave in black powder. Let us consider a variant in which the velocity of layer-by-layer combustion was increased 80-fold compared to the regular value by selecting a proper value of B. The wave velocity–distance diagram is shown in Fig. 6 (curve 6). The steady wave velocity was found to be 2500 m/s. The wave exhibits a classical triangle-shaped Neumann spike (the amplitude of the spike

Table 2. Shock initiation. Variable input parameters for the calculation variants presented in Figs. 6 and 7

Variant no.	Initiation duration, ms	Relative intensity of initiation	Powder granule size, mm	Combustion wave velocity at the end of the charge, m/s
1	30	1.0	0.4	410
2	50	1.2	0.4	750
3	50	1.0	0.2	970
4	40	1.0	0.1	1250
5	50	1.2	0.1	1320

was 3.6 GPa, and the reaction zone thickness was 7 mm).

BLACK POWDER CHARGES IN WEAK CYLINDRICAL SHELLS

The results of experiments with black powder charges confined in long thin-walled tubes made of plastic or copper are presented in [5]. In this case, ignition by electrically heated spiral gives rise to a process of convective combustion that is accompanied by a sonic effect that resembles submachine gun shooting. After the experiment, the tube wall features a series of identical small holes uniformly spaced at 100- to 200-mm intervals, depending on the characteristics of the tube. Ruptures in the shell reflect the specifics of the mechanism of the process: a means of keeping the pressure to below a certain level. On the average, the wave velocity is constant, which was checked for charges shorter than 2 m. Depending on the properties of the shell and charge length, the mean velocity ranged from several meters per second for plastic tubes
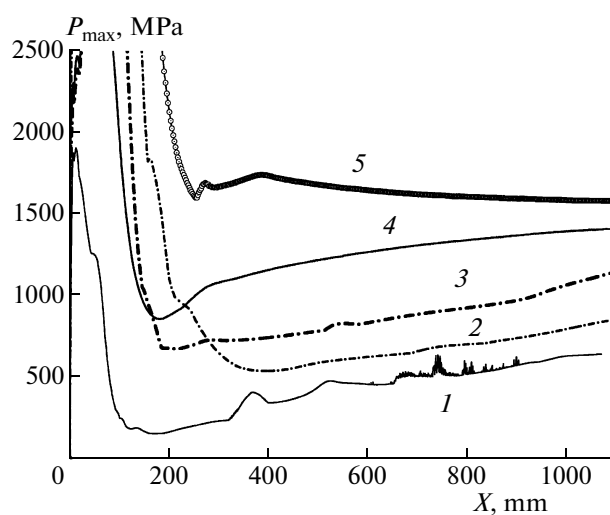

Fig. 7. Maximum pressure in the wave versus the distance for shock initiation: (*1−5*) numbers of the variants specified in Table 2.
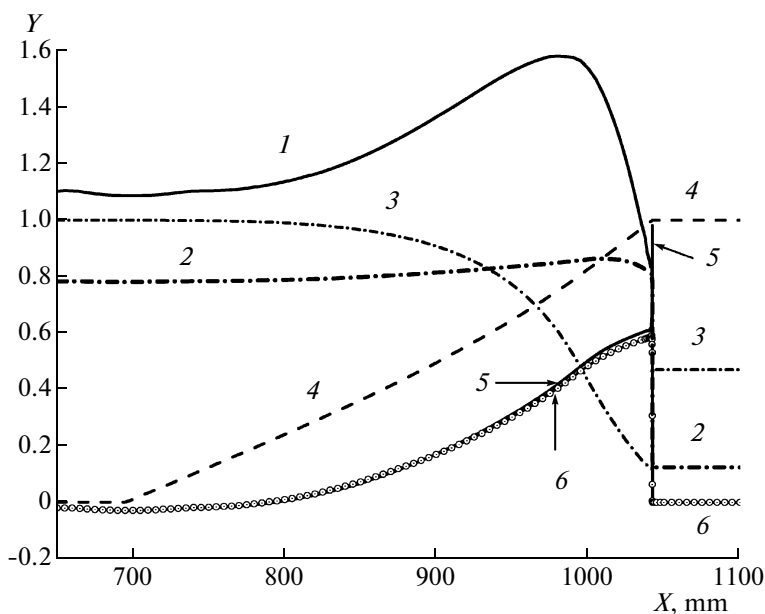
Fig. 8. Space profiles of the key variables at a time 0.726 ms, a combustion front coordinate of 1042.3 mm, and wave velocity of 1325 m/s: (*1*) P (GPa), (*2*) e_g/Q, (*3*) φ, (*4*) d/d_0, (*5*) U_g (km/s), and (*6*) U_c (km/s).
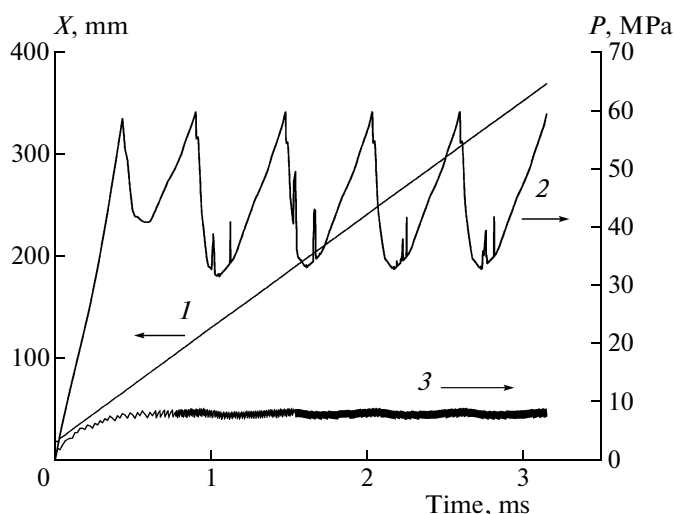

Fig. 9. Pulsating convective combustion in the regime where pulsations fail to reach the head of the combustion wave: (*1*) trajectory of the combustion wave front (*X* axis), (*2*) time evolution of the maximum pressure in the wave, and (*3*) time evolution of the pressure in the wave front (*P* axis).
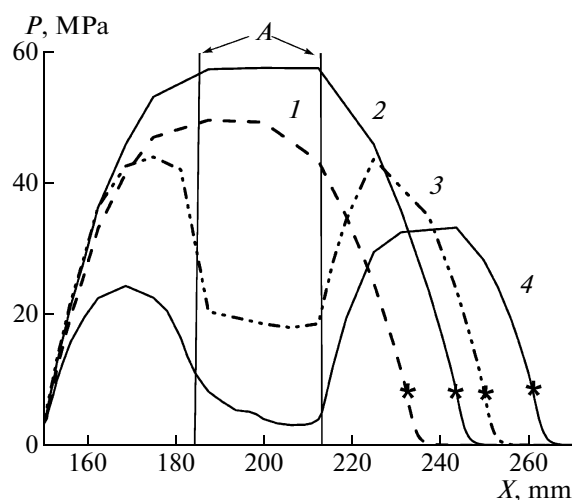
Fig. 10. Pulsating convective combustion for the variant specified in Fig. 9. The development of the rarefaction wave generated by a local rupture of the shell as fixed at various moments of time (in ms): (*1*) 1.91 and (*2*) 2.01 (before the rupture of the shell) and (*3*) 2.07 and (*4*) 2.17 (after the rupture); *A* indicates the boundaries of the local hole in the shell; the asterisk shows the position of the combustion wave front.

to 100 m/s for copper tubes. The process was termed steady-state pulsating convective combustion.

Numerical simulations reproduced the convective combustion of black powder accompanied by pulsations, which are caused by periodic ruptures of the shell. Because of computational difficulties, which were encountered in systematic calculations at various parameters of the shell and black powder, a detailed

analysis of the process will be given elsewhere—here, we limit ourselves to considering the results of immediate bearing on the mechanism of pulsations.

Simulations make it possible to identify two types of interaction of the rarefaction wave generated by the formation of a rupture in the shell with the combustion wave front. The variant when pulsations fail to reach the head of the wave, including the combustion front,
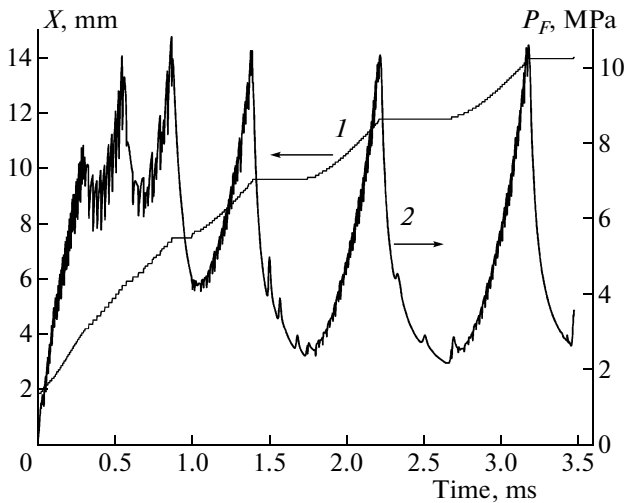
Fig. 11. Pulsating convective combustion with a depression phase: (*1*) trajectory of the combustion wave front (*X* axis) and (*2*) time evolution of the pressure in the wave front (*P_F* axis).

is illustrated in Fig. 9, which shows the trajectory of the wave front, the time evolutions of the maximum pressure and the pressure in the combustion front. After a short transient period, the combustion wave propagated in the steady-state regime at a constant velocity, 112 m/s. Note that the pressure at the combustion front, 8.3 MPa, is substantially lower than the maximum pressure in the wave. Pulsations arise when the maximum pressure reaches the strength limit of

the shell (60 MPa) and a local rupture of the shell forms a hole, through which the combustion products and burning powder granules escape, causing the pressure to drop from its maximum value to ~33.4 MPa. Then, the pressure begins to grow again, approaches its threshold value and the picture repeats itself. Holes in the shell arise in a regular manner at 63-mm intervals, with the period between pulsations being 0.53 ms.

Figure 10 shows space pressure profiles, which demonstrate the development of rarefaction waves generated by local ruptures of the shell and make it possible to understand why pressure pulsations produce virtually no effect on the combustion front trajectory. As can be seen, the distance between the hole and the combustion front is large (~25 mm), and, therefore, the rarefaction wave fails to overtake the front. Thus, periodic ruptures of the shell limit the pressure growth in the wave: were it not for ruptures, pressure growth would cause an acceleration of the combustion front.

A radically different picture is observed for the variant presented in Figs. 11 and 12. In this case, the shell strength was lower, 11.8 MPa; therefore, a rupture in the shell produced a pressure drop in the front from 10 to 2.5 MPa, thereby causing a temporary quenching of combustion. The depression phase lasts for ~0.35 ms. Then, pressure rises in the front and combustion wave propagation resume. The mean velocity of the combustion wave over the segment with pulsations was found to be 25 m/s. That the rarefaction wave strongly affects the combustion front can be accounted for by the fact that the maximum pressure does not signifi-
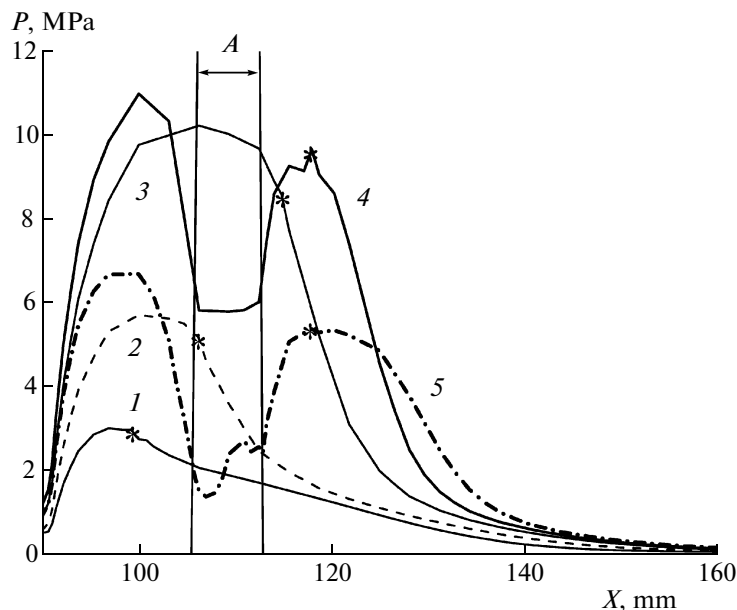

Fig. 12. Pulsating convective combustion with a depression phase. The development of the rarefaction wave generated by a local rupture of the shell as fixed at various instants of time (in ms): (*1*) 1.86, (*2*) 2.02, and (*3*) 2.17 (before the rupture of the shell) and (*4*) 2.23 and (*5*) 2.28 (after the rupture); *A* indicates the boundaries of the local hole in the shell; the asterisk shows the position of the combustion wave front.

cantly exceed the pressure in the combustion wave front and, therefore, each hole is formed only a few millimeters behind the front.

CONCLUSIONS

The explosive and deflagration properties of black powder differ drastically from those of modern propellants and compositions based on ammonium nitrate or ammonium perchlorate. Possessing a high combustibility, black powder is capable of maintaining stable combustion at high velocities in various shells, be it steel shells or thin-walled plastic tubes, without experiencing deflagration-to-detonation transition. It is extremely difficult to detonate black powder, even with a powerful booster detonator.

It is interesting to elucidate whether it is possible to explain the anomalous behavior of black powder within the framework of the existent theoretical notions. In the present work, using numerical simulations, we demonstrated that the main cause of the observed distinctions lies in the burning rate being weakly dependent on the pressure. This feature of black powder combustion is well known [3, 14, 15]; it is explained by the process being controlled by diffusion, although no adequate model of black powder combustion exists.

A theoretical analysis of the processes of convective combustion and deflagration-to-detonation transition in solid energetic materials is enormously simplified by the fact that it can be performed without going into the details of chemical transformations. Success of a numerical simulation largely depends on whether the geometric hypothesis underlying the model works. According to this hypothesis, the intensities of gas and energy release per unit volume occupied by powder granules are determined by the product of the specific surface area of powder granules and the rate of layer-by-layer burning, which is a function of the pressure. The results of the numerical simulations performed in the present work and their qualitative agreement with experimental data obtained over a wide range of initial conditions suggest that this hypothesis generally holds as applied to black powder.

Clearly, a more detailed analysis should take into account factors that were not included into the model, in part because of the lack of required empirical information, for example, on whether the specific surface area of powder granules increases due to their fragmentation during the dynamic densification of powder or on whether the layer-by-layer burning rate is higher because of the porosity of black powder. At the time being, we limited ourselves to increasing the proportionality coefficient in Vieille's law by a factor of ~1.5. It turned out to be sufficient to obtain a close agreement between the predicted and measured characteristics of the convective combustion of a short charge of black powder in a strong shell.

Let us formulate conclusions on the mechanisms and nonideal properties of the considered wave processes.

(1) The process propagating at the velocity of 270 m/s, which is realized in short charges, is ordinary convective combustion. Note, however, that the formation of the rarefaction wave and the linear rise of pressure with time behind the combustion wave front are typical only of black powder and associated with a weak pressure dependence of the layer-by-layer burning rate. Indeed, if the pressure exponent n were close to unity, the pressure behind the combustion front would rise exponentially and the effect of the rarefaction wave would be screened.

(2) The process that propagates at the velocity of 400−440 m/s, which is observed in long charges irrespective of the initiation mode, is also convective combustion. The combustion wave velocity, which remains virtually constant after a transient period despite pressure rise, is determined by the properties of the developed densification zone (plug) formed ahead of the front. The large span of the plug and the inability of the combustion front to overcome it are also consequences of the pressure exponent being small.

(3) The process propagating at the velocity of 1100−1300 m/s, which is realized due to special shock initiation, can be classified as nonideal detonation, which has no time to develop into Chapman−Jouguet detonation because of a very large span of the reaction zone. In a strong steel shell, the wave propagates through meter-long charges at nearly constant velocity of the front. Note that this velocity is nearly twice as low as the thermodynamically calculated velocity of the ideal detonation of black powder.

(4) For steady convective combustion with pulsations generated by periodic ruptures of a weak shell, numerical simulations made it possible to identify two different mechanisms of pulsations. The mechanism by which the rarefaction wave generated by a local rupture in the shell entrains the combustion front, thereby suspending its propagation for a time, was already discussed in [5]. According to the new mechanism, pulsations fail to reach the combustion front because of a large distance between the combustion front and the point of maximum pressure in the combustion wave. The two factors, a weak dependence of the burning rate on the pressure and a high heat conduction rate due to the deposition of combustion products on powder particles, substantially attenuate the effect of pulsations on the combustion front, thereby ensuring a high stability of the convective combustion of black powder under conditions of periodically occurring ruptures of the shell.

Studies of the deflagration and detonation properties of black powder can be of interest for interpretation of nonideal explosive processes, which have been discovered recently to occur in a number of pyrotech-

nic compositions, for example, aluminum–sulfur mixtures [19].

ACKNOWLEDGMENTS

REFERENCES

1. G. Kast, *Explosive Substances and Ignition Means* (GKhTI, Moscow, 1932) [in Russian].

2. N. A. Shilling, *A Course on Black Powders* (GIOP, Moscow, 1940) [in Russian].

3. O. I. Leipunskii, Zh. Fiz. Khim. **34**, 177 (1960).

4. A. F. Belyaev and R. Kh. Kurbangalina, Zh. Fiz. Khim. **38**, 579 (1964).

5. B. S. Ermolaev, A. A. Sulimov, V. A. Foteenkov, et al., Fiz. Goreniya Vzryva **16** (3), 24 (1980).

6. V. A. Foteenkov, A. I. Korotkov, B. S. Ermolaev, et al., Fiz. Goreniya Vzryva **18** (2), 137 (1982).

7. V. A. Foteenkov, A. A. Sulimov, and A. I. Korotkov, in *Proc. 16th Intern. Pyrotechnics Seminar* (Billdall, Hansson Pyrotech AB, 1991), Paper No. 9, p. 121.

8. B. S. Ermolaev, A. A. Belyaev, and A. A. Sulimov, Khim. Fiz. **23** (1), 62 (2004).

9. J. Bdzil, R. Menikoff, S. Son, et al., Phys. Fluids **11**, 378 (1999).

10. S. B. Victorov, in *Proc. 12th Intern. Detonation Symp.* (ONR, Arlington, 2002), p. 369.

11. S. B. Viktorov, S. A. Gubin, I. V. Maklashova, et al., Khim. Fiz. **24** (12), 22 (2005).

12. S. B. Victorov and S. A. Gubin, in *Proc. 13th Intern. Detonation Symp.* (ONR, Arlington, 2006), Paper 148.

13. B. S. Ermolaev, B. A. Khasainov, and H.-N. Presles, in *Proc. Europyro 2007 - 34th IPS*, Vol. 1 (AFP, Paris, 2007), p. 323.

14. A. P. Glazkova and I. A. Tereshkin, Zh. Fiz. Khim. **35**, 1622 (1961).

15. A. F. Belyaev, A. I. Korotkov, A. K. Parfenov, et al., Zh. Fiz. Khim. **37**, 150 (1963).

16. M. E. Serebryakov, *Internal Ballistics* (Oborongiz, Moscow, 1949), p. 41 [in Russian].

17. A. A. Sulimov and B. S. Ermolaev, Khim. Fiz. **16** (9), 51 (1997).

18. B. S. Ermolaev and A. A. Sulimov, in *Proc. of the Cinquieme Symp. Intern. Sur Hautes Pressions Dynamiques (HDP V)* (AFP, Paris, 2003), p. 15.

19. A. Yu. Dolgoborodov, A. N. Streletskii, M. N. Makhov, et al., Khim. Fiz. **25** (12), 40 (2007) [Russ. J. Phys. Chem. B **1**, 606 (2007)].